AHMAD, Z., HASAN, M.J. and KIM, J.-M. 2022. Transfer learning with 2D vibration images for fault diagnosis of bearings under variable speed. In *Abraham, A., Gandhi, N., Hanne, T., Hong, T.-P., Rios, T.N. and Ding, W. (eds.) Intelligent systems design and applications: proceedings of 21st International conference on intelligent systems design and applications (ISDA 2021), 13-15 December 2021, [virtual event]*. Lecture notes in networks and systems, 418. Cham: Springer [online], pages 154-164. Available from: https://doi.org/10.1007/978-3-030-96308-8_14

Transfer learning with 2D vibration images for fault diagnosis of bearings under variable speed.

AHMAD, Z., HASAN, M.J. and KIM, J.-M.

2022

Transfer-Learning with 2D Vibration Images for Fault Diagnosis of Bearings under Variable Speed

Zahoor Ahmad[1], Md Junayed Hasan[1], and Jong-Myon Kim[1*]

[1] Department of Computer Engineering, University of Ulsan, Ulsan 44610, Republic of Korea
jmkim07@ulsan.ac.kr

Abstract. One of the most critical assignments in fault diagnosis is to decide the finest set of features by evaluating the statistical parameters of the time-domain signals. However, these parameters are vulnerable under variable speed conditions to capture the dynamic attributes of various health types. Therefore, this paper proposes a vibration imagining-based diagnosis approach for bearing under variable speed conditions. First, a Discrete Cosine Stockwell Transformation (DCST) coefficient-based preprocessing step is proposed to create an identical health pattern for variable speed conditions. Then, from that 2D coefficient matrix, a vibration image is created to capture those health patterns into grayscale. Finally, a Transfer Learning embedded Convolutional Neural Network (TL-CNN) is proposed to inspect the comprehensive structure of the 2D vibration images for final classification. The experimental results show that the proposed method achieved 100% classification accuracy on a publicly available dataset.

Keywords: Bearing, Condition monitoring, Convolutional Neural Network, Stockwell Transformation, Transfer Learning.

1 Introduction

Rotating machinery plays an increasingly significant role in many industries [1, 2]. To reduce the economic losses and increase safety, fault diagnosis is of main importance [3]. Rolling element bearing is the most vital component of the rotating machinery. Rolling element bearings operate in harsh working environments, thus, these components become the primary reasons for the sudden failures of these machinery [1], and create huge economic fatalities [4]. In the past decades, industries focused on robust condition monitoring methods [5]. Moreover, to get some meaningful insights from the signals for fault diagnosis, throughout these years, researchers have relied upon several signal processing techniques, such as Fast Fourier Transformation (FFT) [6], Empirical Mode Decomposition [7], Energy Entropy [8], Wavelet Packet Decomposition [9], Empirical Wavelet Transformation [10], Variational Mode Decomposition [11], Continuous Wavelet Transform [12], etc. These approaches provide satisfactory performance under static working conditions of rotary machines. However, due to tension, clearance, and inconsistent working conditions, the obtained signals from these machines are non-linear and non-stationary in nature, which creates difficulties to extract and analyze the fault feature information [13–15]. Specifically, via the popular feature extraction

*Corresponding author.

methods, it becomes very challenging to distinguish the fault characteristics for variable working conditions [16–18]. Therefore, it is inescapable to come up with a new and effective signal processing technique through which fault signature exploration can become reliable for different speed conditions [19,20]. For the following 2 benefits of the Stockwell Transformation (ST), in this study, ST based preprocessing step is considered to create the health pattern from the vibration signals: (i) it has better immunity to ample noise, and (ii) it can obtain good resolutions from the signals both at low and high frequencies. Thus, the contributions of this study can be discussed as follows.

(1) To capture the information of variable speed conditions from the vibration signals both at low and high frequencies, A 2D coefficient-based DCST is proposed as the signal preprocessing step.

(2) To utilize CNN efficiently, the DCST 2D coefficients are converted into grayscale Vibration Images (VI).

(3) A TL embedded CNN is offered for the diagnosis purpose. The proposed method (VI + CNN-TL) is appropriately supported with extensive experimentations, which supports the capability of the proposed methodology over existing state-of-art approaches.

The rest of the paper is arranged as follows: Section 2 explains the proposed methodology, section 3 describes the details of the considered dataset along with the experimental analysis, and finally, section 4 concludes this study.

2 Proposed Approach

The proposed approach consist of 3 steps: source task, transfer task, and target task. In the source task, first, an invariant scenario is created with the help of DCST based 2D coefficient analysis. With this preprocessing step, we have obtained similar patterns for similar health conditions under variable speeds. Then, this 2D coefficient matrix is converted into grayscale VI. Finally, these images are fed to the proposed neural network for condition classification. In the source task, we have considered the dataset from a certain speed to train the network for attaining transferrable knowledge. Then, the transfer task passes that knowledge to the target network. Therefore, in the target task, the data obtained from different speed conditions are used to examine the diagnostic performance. The overall approach is illustrated in Fig. 1.

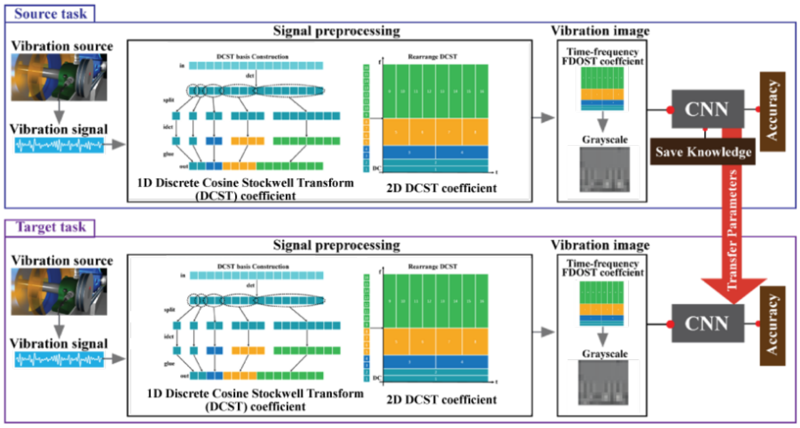

Fig. 1. The block diagram of proposed approach.

2.1 Data Preprocessing based on Stockwell Transformation

The vibration signal obtained from the bearing contains fault-related information and additive noise from the surrounding [21]. Therefore, it is difficult to extract fault-related information from these signals in either time or frequency domain[22]. To handle this issue, Discrete Cosine Stockwell Transform (DCST) has been proposed as the preprocessing step in this work. First, the raw signals are segmented into smaller sizes by the adjustable overlapping sliding window [17]. Each of these segments contains the data points from at least one revolution [23]. After that, on each segmented signal, we have applied DCST to obtain the 1D coefficients.

Stockwell Transformation (ST) acts as a hybrid between Gabor, and Wavelet transformation [24]. By principle, it exhibits the decomposition techniques of a signal based on an orthogonal basis [25]. In this study, instead of that orthogonal basis, the Cosine Transform basis is considered. It follows the principles of the orthogonal basis, however, instead of using Discrete Fourier Transform (DFT), it considers Discrete Cosine Transform (DCT) [26]. DCT is a linear and invertible function.

$$f : \mathrm{R}^N \to \mathrm{R}^N \qquad (1)$$

Where R signifies to the set of real numbers. In general, the following equation is the standard form of DCT, known as type – II DCT.

$$X_k = \sum_{n=0}^{N-1} x_n \cos\left[\frac{\pi}{N}\left(n+\frac{1}{2}\right)k\right] \qquad (2)$$

where N real numbers $x_0, ..., x_{N-1}$ are converted into $X_0, ..., X_{N-1}$ real numbers and k holds the values $0, 1, ..., N-1$. The type-II DCT is precisely corresponding to a DFT of $4N$ (up to a complete measure aspect of 2) with even symmetry. To satisfy the boundary condition for type-II DCT, x_N is even around $n = -\frac{1}{2}$ and even around $n = -\frac{N-1}{2}$; x_k is even around $k = 0$ and odd around $k = N$. Therefore, DCT can preserve concentrated histograms information more than DFT from the input signal.

Finally, to simplify the interpretation of the DCST coefficient, it is rearranged into the phase space [24]. The rearrangement process is visually described in Fig. 2(b).

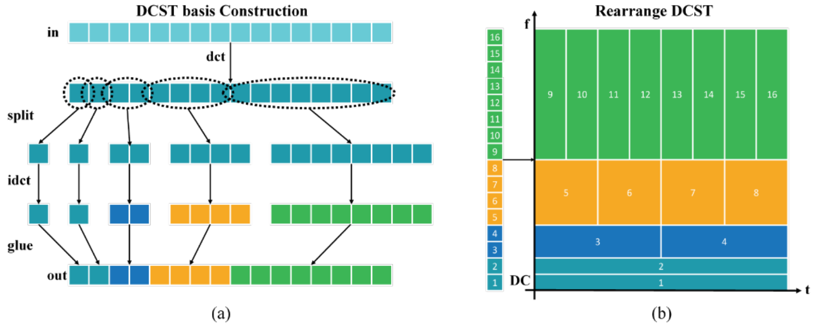

Fig. 2. (a) DCST basis construction process, **(b)** for 2-dimensional imaging, the rearrangement process from DCST constructed output.

2.2 Vibration Imaging

The formulation of Vibration Imaging (VI) is implemented into two steps to discover the patterns of different health types, i.e.,

(1) The time-domain vibration signals are preprocessed by the DCST coefficient, and thus, 2D time-frequency images are achieved. These 2D images preserve the data about the energy distribution across the time-frequency planes [27].

(2) The resulting time-frequency images are then transformed into gray-scale images ($256 \times 256 \times 1$)[28]. Thus, it adds computational benefits for neural network-based analysis [29].

2.3 Transfer Learning-based Convolutional Neural Network Architecture

To implement the knowledge transfer between the source and the target task, we have utilized the Le-Net5 [30] based Convolutional Neural Network (CNN) architecture. The proposed architecture of the CNN is highlighted in Fig. 3. For training purposes, Stochastic Gradient Descent (SGD) [31] is used as the optimizer. Additionally, 0.01 learning rate and SoftMax classifier is used to complete the forward, and backward propagation. For the target task, weights till the bottom neck layer of the source network are transferred for the final diagnosis purpose.

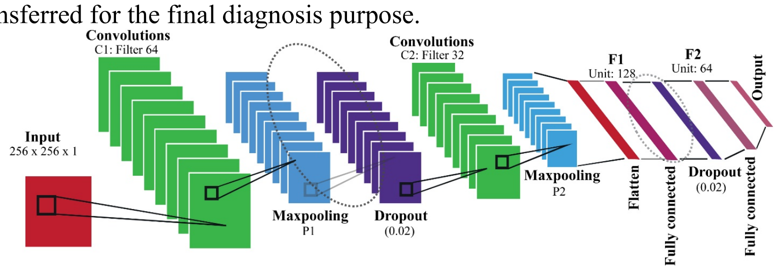

Fig. 3. The proposed CNN architecture.

2.4 Performance Evaluation

To evaluate the performance of the proposed approach, F1 score (F1), and Accuracy (A) is calculated by the following equations:

$$F1 = \left[\frac{2TP}{2TP + FN + FP} \times 100 \right] \% \quad (3)$$

$$A = \left[\frac{(TP + TN)}{(TP + FP + TN + FN)} \times 100 \right] \% \quad (4)$$

Moreover, for the source task, to observe the bias-variance tradeoff, the model is trained till 6,000 epochs. Therefore, the performance of the loss function can be observed. Consequently, to eliminate the bias from the data, a 6-Fold Cross-Validation (6-CV) [32] is used.

3 Experimental Result Analysis

3.1 Dataset Description and Experimental Setup

To evaluate the performance of the proposed model, a publicly available dataset from the Case Western Reserve University (CWRU) Bearing Datacenter [33] is used. The experimental setup of the testbed of this dataset is given in Fig. 4.

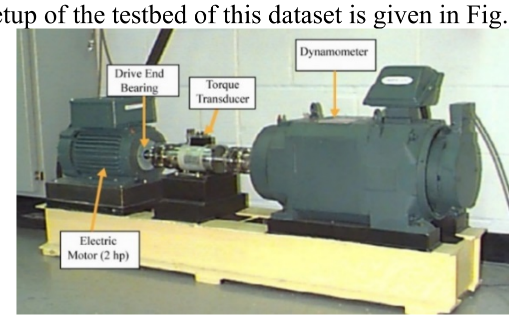

Fig. 4. Experimental set up by Case Western Reserve University[33].

This dataset is composed of vibration signals of 12,000 Hz from the drive-end bearing. The details of the considered working conditions from this dataset are highlighted in Table 1.

Table 1. Details of the dataset collected from CWRU bearing data center

Working Condition (WC)	Health Type	Shaft Speed (RPM)	Load	Crack Size Length (inches)
1	Normal	1797	0	-
	Inner Raceway		0	0.007
	Outer Raceway		0	0.007

	Ball		0	0.007
2	Normal	1772	1	-
	Inner Raceway		1	0.007
	Outer Raceway		1	0.007
	Ball		1	0.007

Before supplying the proposed diagnostic model, we ensured that every health type has an equal number of samples, and there is no missing value in it. For the final analysis, 2 experiments are performed. In experiment 1, Working Condition (WC) 1 is used as the source task, and WC 2 is utilized as the target task. In experiment 2, WC 2 is considered as the source, and WC 1 is considered as the target task. The details of the data division for both experiments are given in Table 2.

Table 2. Data Division

Source Task	**WC**	Training (90%) Samples		Test (10%) Samples	Samples/Health Type
		Training (80%)	Validation(20%)		
	1	1944	216	240	60
	2	1944	216	240	60
Target Task	**WC**	Training (90%) Samples		Test (10%) Samples	Samples/Health Type
		Training (80%)	Validation(20%)		
	1	324	36	2040	510
	2	324	36	2040	510

3.2 Result Analysis

After applying the DCST based preprocessing step, and 2D coefficient-based vibration imaging process, the obtained patterns for each health type of both the working conditions are given in Fig. 5. From this Figure, we can observe that, for all the health types, there are distinguishable patterns. Moreover, for a similar type of health type, the patterns are identical for different speed conditions. For example, for IR, the pattern is similar for WC1, and WC2. Similarly, it is true for all other health types. Therefore, our proposed preprocessing step can successfully create the invariant scenario for variable working conditions.

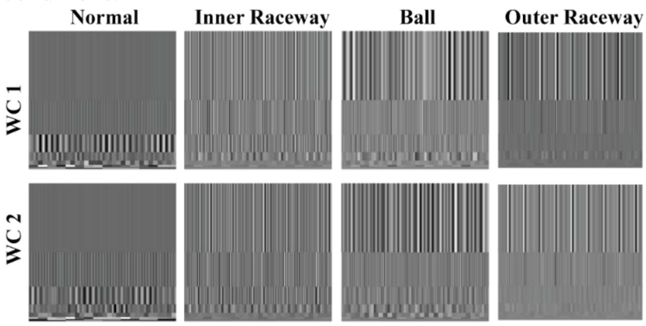

Fig. 5. Vibration images from different health types.

Once the patterns are obtained, we have conducted both experiments. For each case, we have achieved 100% accuracy. In Table 3, the details of this experimental analysis are depicted.

Table 3. Analytical performance.

Experiment	Source Task	Target Task	Health Type	F1 (%)	A(%)
1	WC 1	WC 2	N	100	**100**
			IR	100	
			OR	100	
			B	100	
2	WC 2	WC 1	N	100	**100**
			IR	100	
			OR	100	
			B	100	

To demonstrate the details of these experimental analyses, experiment 1 is further investigated. From the source task of experiment 1, the graph of the loss function and the last layer feature separability of the source acquired by t-SNE [21], are highlighted in Fig. 6.

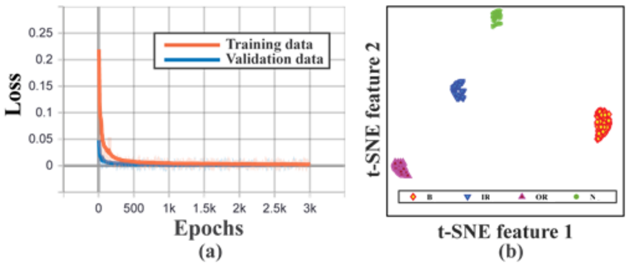

Fig. 6. For experiment 1 – source task (WC 1) (a) loss function, (b) bottom neck layer features by t-SNE.

The TL-based approach learns faster with a smaller amount of data because the trained weights of the source task are used to adjust the network parameters for the target task. To prove this argument, we have considered the target task of experiment 1. For this experiment, first, we have trained the proposed CNN architecture with WC 2 from scratch without the weights from the source task. Therefore, we have observed the convergence rate of the loss function. After that, we have used the weights from the source task, and train the target task according to Experiment 1. Here also we have observed the loss function. From Fig. 7, we can perceive that for this TL-based approach, our model achieved 100% training accuracy in a very short amount of time (at least 6X times faster).

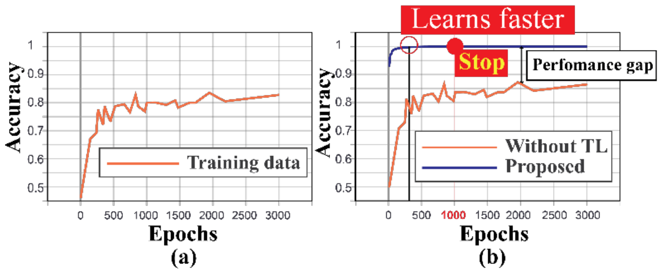

Fig. 7. (a) The training accuracy achieved with WC 2: target task for 3,000 epochs with no TL, and (b) the training accuracy without TL vs. with TL (proposed).

Additionally, several comparisons are made to substantiate the dominance of our proposed method. In all cases, it outperforms the existing approaches. Details of the comparative analysis are given in Table 4.

Table 4. Comparison Analysis

Method	**Experi-ment**	**A (%)**	**Improvement (%)**
FFT + CNN - TL	1	97.2	**2.8**
	2	96.5	**3.5**
RAW + CNN – TL [34]	1	92.1	**7.9**
	2	92.3	**7.7**

4 Conclusions

This paper proposes a TL-CNN-based approach for condition monitoring of bearing with different speed conditions. With the help of DCST, we have created the invariant scenario from variable working conditions. Thus, the feature similarity comes into the source and target task datasets. Therefore, by utilizing this similarity in patterns, TL based approach perfectly utilized the power of the proposed CNN architecture for diagnosing the health types of bearing. By outperforming the conventional approaches, it stands as state-of-art among all the proposed approaches proposed in this dissertation. However, this method has the limitations of explanation ability and interpretability from the statistical point of view related to the feature spaces. Therefore, the future direction of this work is to explore the possibilities of explanations and interpretations for a complete explainable model.

Acknowledgments. This research was financially supported by the Ministry of Small and Medium-sized Enterprises(SMEs) and Startups(MSS), Korea, under the "Regional Specialized Industry Development Plus Program(R&D, S3092711)" supervised by the Korea Institute for Advancement of Technology(KIAT).

References

1. Yan, X., Jia, M.: A novel optimized SVM classification algorithm with multi-domain feature and its application to fault diagnosis of rolling bearing. Neurocomputing. 313, 47–64 (2018).
2. Lei, Y., He, Z., Zi, Y.: A new approach to intelligent fault diagnosis of rotating machinery. Expert Syst. Appl. 35, 1593–1600 (2008).
3. Yan, X., Liu, Y., Jia, M., Zhu, Y.: A multi-stage hybrid fault diagnosis approach for rolling element bearing under various working conditions. IEEE Access. 7, 138426–138441 (2019).
4. Cui, L., Huang, J., Zhang, F.: Quantitative and localization diagnosis of a defective ball bearing based on vertical–horizontal synchronization signal analysis. IEEE Trans. Ind. Electron. 64, 8695–8706 (2017).
5. Rai, A., Kim, J.-M.: A novel health indicator based on the Lyapunov exponent, a probabilistic self-organizing map, and the Gini-Simpson index for calculating the RUL of bearings. Measurement. 108002 (2020).
6. Shao, S.-Y., Sun, W.-J., Yan, R.-Q., Wang, P., Gao, R.X.: A deep learning approach for fault diagnosis of induction motors in manufacturing. Chinese J. Mech. Eng. 30, 1347–1356 (2017).
7. Sun, Y., Li, S., Wang, X.: Bearing fault diagnosis based on EMD and improved Chebyshev distance in SDP image. Measurement. 109100 (2021).
8. Ali, J. Ben, Fnaiech, N., Saidi, L., Chebel-Morello, B., Fnaiech, F.: Application of empirical mode decomposition and artificial neural network for automatic bearing fault diagnosis based on vibration signals. Appl. Acoust. 89, 16–27 (2015).
9. Zhao, L.-Y., Wang, L., Yan, R.-Q.: Rolling bearing fault diagnosis based on wavelet packet decomposition and multi-scale permutation entropy. Entropy. 17, 6447–6461 (2015).
10. Qiao, Z., Liu, Y., Liao, Y.: An improved method of EWT and its application in rolling bearings fault diagnosis. Shock Vib. 2020, (2020).
11. Gu, R., Chen, J., Hong, R., Wang, H., Wu, W.: Incipient fault diagnosis of rolling bearings based on adaptive variational mode decomposition and Teager energy operator. Measurement. 149, 106941 (2020).
12. Cheng, Y., Lin, M., Wu, J., Zhu, H., Shao, X.: Intelligent fault diagnosis of rotating machinery based on continuous wavelet transform-local binary convolutional neural network. Knowledge-Based Syst. 216, 106796 (2021). https://doi.org/https://doi.org/10.1016/j.knosys.2021.106796.
13. Kang, M., Kim, J., Kim, J.M., Tan, A.C.C., Kim, E.Y., Choi, B.K.: Reliable fault diagnosis for low-speed bearings using individually trained support vector machines with kernel discriminative feature analysis. IEEE Trans. Power Electron. 30, 2786–2797 (2015). https://doi.org/10.1109/TPEL.2014.2358494.
14. Sohaib, M., Kim, C.-H., Kim, J.-M.: A Hybrid Feature Model and Deep-Learning-Based Bearing Fault Diagnosis. Sensors. 17, 2876 (2017). https://doi.org/10.3390/s17122876.
15. Rai, A., Upadhyay, S.H.: A review on signal processing techniques utilized in the fault diagnosis of rolling element bearings. Tribol. Int. 96, 289–306 (2016).
16. Khan, S.A., Kim, J.-M.: Rotational speed invariant fault diagnosis in bearings using vibration signal imaging and local binary patterns. J. Acoust. Soc. Am. 139, EL100–

EL104 (2016). https://doi.org/10.1121/1.4945818.
17. Hasan, M.J., Islam, M.M.M., Kim, J.M.: Acoustic spectral imaging and transfer learning for reliable bearing fault diagnosis under variable speed conditions. Meas. J. Int. Meas. Confed. 138, 620–631 (2019). https://doi.org/10.1016/j.measurement.2019.02.075.
18. Islam, M.M.M., Myon, J.: Time–frequency envelope analysis-based sub-band selection and probabilistic support vector machines for multi-fault diagnosis of low-speed bearings. J. Ambient Intell. Humaniz. Comput. 0, 0 (2017). https://doi.org/10.1007/s12652-017-0585-2.
19. Qu, J., Zhang, Z., Gong, T.: A novel intelligent method for mechanical fault diagnosis based on dual-tree complex wavelet packet transform and multiple classifier fusion. Neurocomputing. 171, 837–853 (2016).
20. Chen, G., Liu, F., Huang, W.: Sparse discriminant manifold projections for bearing fault diagnosis. J. Sound Vib. 399, 330–344 (2017).
21. Hasan, M.J., Sohaib, M., Kim, J.-M.: A Multitask-Aided Transfer Learning-Based Diagnostic Framework for Bearings under Inconsistent Working Conditions. Sensors. 20, 7205 (2020).
22. Zhao, M., Kang, M., Tang, B., Pecht, M.: Multiple Wavelet Coefficients Fusion in Deep Residual Networks for Fault Diagnosis. IEEE Trans. Ind. Electron. 66, 4696–4706 (2019). https://doi.org/10.1109/TIE.2018.2866050.
23. Hasan, M.J., Sohaib, M., Kim, J.-M.: An Explainable AI-Based Fault Diagnosis Model for Bearings. Sensors. 21, 4070 (2021).
24. Stockwell, R.G.: A basis for efficient representation of the S-transform. Digit. Signal Process. A Rev. J. 17, 371–393 (2007). https://doi.org/10.1016/j.dsp.2006.04.006.
25. Stockwell, R.G.: Why use the S-Transform? Fields Inst. Commun. 52, 279–309 (2007).
26. Battisti, U., Riba, L.: Window-dependent bases for efficient representations of the Stockwell transform. Appl. Comput. Harmon. Anal. 40, 292–320 (2016). https://doi.org/10.1016/j.acha.2015.02.002.
27. Türk, Ö., Özerdem, M.S.: Epilepsy detection by using scalogram based convolutional neural network from EEG signals. Brain Sci. 9, 115 (2019).
28. Bala, R., Braun, K.M.: Color-to-grayscale conversion to maintain discriminability. In: Color Imaging IX: Processing, Hardcopy, and Applications. pp. 196–202. International Society for Optics and Photonics (2003).
29. Wang, J., Mo, Z., Zhang, H., Miao, Q.: A deep learning method for bearing fault diagnosis based on time-frequency image. IEEE Access. 7, 42373–42383 (2019).
30. LeCun, Y.: LeNet-5, convolutional neural networks. URL http//yann. lecun. com/exdb/lenet. 20, 5 (2015).
31. Bottou, L.: Stochastic gradient descent tricks. In: Neural networks: Tricks of the trade. pp. 421–436. Springer (2012).
32. Browne, M.W.: Cross-validation methods. J. Math. Psychol. 44, 108–132 (2000).
33. University, C.W.R.: Bearing Data Center Website, http://csegroups.case.edu/bearingdatacenter/pages/download-data-file.
34. Zhang, R., Tao, H., Wu, L., Guan, Y.: Transfer Learning with Neural Networks for Bearing Fault Diagnosis in Changing Working Conditions. IEEE Access. 5, 14347–14357 (2017). https://doi.org/10.1109/ACCESS.2017.2720965.